Chapter 3
Stability Analysis for Rotary-Wing Aircraft

3.1 Introduction

With the flight dynamic modeling from Chap. 2, the natural next step is to conduct trim analysis. Trim is a state in which force and moment equilibrium are maintained. Trim analysis is the basis of many rotary-wing aircraft studies, including performance and stability analysis, control system design, handling qualities assessment, and software-in-the-loop simulation.

During the linearization process, small perturbation can be applied to the trimmed states to extract the linearized model. All elements in the linearized model can be grouped into four categories: gravity terms, kinematic terms, stability derivative terms, and control derivative terms. Focus is given on a sanity check of these terms. At the end of the chapter, three examples will be provided on the dynamic stability study of the rotary-wing aircraft.

3.2 Trim

Trim calculation can be conducted analytically or numerically. A good illustration of an analytical trim calculation can be referred to in [84]. While analytical trim calculation may provide insight on critical forces and moments acting on the rotary-wing aircraft, its application is restricted to simplified analytical equations or special flight conditions in which great simplifications are required.

It may be noticed by readers that the mathematical modeling detailed in Chap. 2 tends to be matrix-centric and can thus be easily implemented in *Matlab*™. As a result, numerical trim calculation can be conducted based on the *Trim* command available in *Matlab*™. A description of this command can be referred in the *Simulink*™ User Manual.

B. Ren et al., *Modeling, Control and Coordination of Helicopter Systems*,
DOI 10.1007/978-1-4614-1563-3_3, © Springer Science+Business Media, LLC 2012

In this section, the procedure for numerical trim calculation is outlined based on the Newton method. The procedure can be implemented in the *Matlab*™ environment, as well as other programming languages like C. Compared to the *Trim* command in *Matlab*™, this set of procedures can provide greater flexibilities in fine-tuning parameters related to convergence and its speed.

Typical difficulties related to the Newton method include the existence of multiple equilibria, computation and singularity of the Jacobian matrix, and closeness of the initial guess to the final converged solution. In the application of rotary-wing aircraft, one possible case for multiple equilibria occurs when the blade sectional angle of attack gets close to the stall region. Here, a single value of lift coefficient may correspond to two angles of attack near to each other. A remedy is thus to smooth out the lift coefficient curve. Generating the Jacobian matrix may not be a big problem as the trim problem only involves a small number of trim variables (typically six) and the matrix can be obtained through numerical perturbation. In terms of the initial guess, one can always start with hover condition and increase flight speed in a comfortably small step. Singularity of the Jacobian matrix may occur at extreme flight conditions like flying at V_{ne} (never exceed speed). For flight conditions close to the boundaries of the flight envelope, professional judgement needs to be made to determine whether the failure to converge is due to numerical reasons or physical causes.

As a general formulation, suppose that the dynamic system can be represented as follows:

$$\dot{X} = f(X, U) \tag{3.1}$$

Here, X can be states from the general six degree-of-freedom equations of motion, blade flapping equations, rotor rotational degree-of-freedom, or dynamics involving flight control system. U are either control variables in general or trim variables in the trim problem.

The procedures using Newton's method are described as follows:

1. Set flight condition X.
2. Set trim targets Y which can be a subset of $\dot{X}$.
3. Set trim variables U and associated perturbation Δh.
4. Set initial conditions for trim variables U_0 and run system (3.1) to obtain Y_0.
5. Vary one trim variable at a time as $U(i) + \Delta h(i)$ and run the full system to obtain Y^i.
6. Form the Jacobian matrix J:

$$J(:, i) = \frac{Y^i - Y_0}{\Delta h(i)} \tag{3.2}$$

7. Obtain J^{-1}.

Table 3.1 Setting on trim variables and trim targets

Trim flight conditions	Trim variables	Trim targets
Steady level flight or hover	$\theta_c, \theta_{1c}, \theta_{1s}, \theta_{c_{\text{tr}}}, \phi, \theta$	$\dot{u}, \dot{v}, \dot{w}, \dot{p}, \dot{q}, \dot{r}$
Climb or descent	$\theta_{1c}, \theta_{1s}, \theta_{c_{\text{tr}}}, \phi, \theta, \gamma_{\text{v}}$	$\dot{u}, \dot{v}, \dot{w}, \dot{p}, \dot{q}, \dot{r}$
Autorotation	$\theta_c, \theta_{1c}, \theta_{1s}, \theta_{c_{\text{tr}}}, \phi, \theta$	$\dot{u}, \dot{v}, \dot{w}, \dot{p}, \dot{q}, \dot{r}$
	γ_{v}	$\dot{\Omega}_{\text{rotor}}$
Coordinated turn	$\theta_c, \theta_{1c}, \theta_{1s}, \theta_{c_{\text{tr}}}, \phi, \theta$	$\dot{u}, \dot{v}, \dot{w}, \dot{p}, \dot{q}, \dot{r}$
Longitudinal static stability	$\theta_{1c}, \theta_{1s}, \theta_{c_{\text{tr}}}, \phi, \theta, \gamma_{\text{v}}$	$\dot{u}, \dot{v}, \dot{w}, \dot{p}, \dot{q}, \dot{r}$
Lateral static stability	$\theta_{1c}, \theta_{1s}, \theta_{c_{\text{tr}}}, \phi, \theta, \gamma_{\text{h}}$	$\dot{u}, \dot{v}, \dot{w}, \dot{p}, \dot{q}, \dot{r}$

8. Set the update of U:

$$U_{\text{new}} = U_{\text{old}} - J^{-1}(Y_{\text{old}} - Y) \tag{3.3}$$

9. Run the full system to obtain Y_{new}.
10. Test whether $||Y_{\text{new}} - Y|| < \epsilon$. If not, go back to Step 8.

Astute readers may realize that the above procedures do not strictly follow the classical Newton method. It is in fact a variant of the Newton method called the Chord method. The advantage of the Chord method is that it only requires us to compute the Jacobian matrix once, thus saving considerable computational cost. However, while the Newton method can guarantee quadratic convergence, the Chord method can only achieve linear convergence.

A collection of trim variables and trim targets at various trimmed flight conditions is provided in Table 3.1 [14]:

In Table 3.1, γ_{h} and γ_{v} represent horizontal and vertical flight path angles, respectively. In some trim conditions, collective pitch θ_0 is not one of the trim variables as it is set by a predefined value.

3.3 Linearization

The process of linearization is based on small perturbation theory in which a variable is the sum of its nominal value plus a perturbation. For example, pitch attitude, θ, is written as

$$\theta = \theta_0 + \Delta\theta \tag{3.4}$$

In another example, the total force acting along x-axis in body frame, X, can be expressed as

$$X = X_0 + \Delta X \tag{3.5}$$

The incremental force ΔX can be further extended with the following linear approximation:

$$\Delta X = X_u \Delta u + X_w \Delta w + X_q \Delta q + X_{\theta_c} \Delta\theta_c + X_{\theta_{1s}} \Delta\theta_{1s} \tag{3.6}$$

In the above expression, the terms (X_u, X_w, X_q) are called stability derivatives, while the remaining terms (X_{θ_c}, $X_{\theta_{1s}}$) are referred to as control derivatives. Both stability and control derivatives are first order partial derivatives. While these derivatives can also be obtained through analytical investigation [84], they can be computed by numerical perturbation. For example, drag damping X_u is

$$X_u = \frac{\partial X}{\partial u} \cong \frac{X(U_0 + \Delta u) - X(U_0)}{\Delta u} \tag{3.7}$$

The product from the linearization process is a linearized system with respect to a reference flight condition in the following form:

$$\dot{x} = Ax + Bu \tag{3.8}$$

with states $x^{\mathrm{T}} = [u,\ w,\ q,\ \theta,\ v,\ p,\ r,\ \phi]$ and control inputs $u^{\mathrm{T}} = [\theta_c, \theta_{1s}, \theta_{1c}, \theta_{c_{\mathrm{tr}}}]$. Notice that, for simplicity, the symbol Δ is not explicitly included in the increments of variables. Matrix A is made of four parts: longitudinal dynamic A_{long}, lateral dynamics A_{lat}, longitudinal/lateral coupling $A_{\mathrm{long/lat}}$, and lateral/longitudinal coupling $A_{\mathrm{lat/long}}$:

$$A = \begin{bmatrix} A_{\mathrm{long}} & A_{\mathrm{long/lat}} \\ A_{\mathrm{lat/long}} & A_{\mathrm{lat}} \end{bmatrix} \tag{3.9}$$

General forms of these four sub-matrices are provided:

$$A_{\mathrm{long}} = \begin{bmatrix} \frac{X_u}{m} & \frac{X_w}{m} & \frac{X_q}{m} - W_0 & -g\cos\theta_0 \\ \frac{Z_u}{m} & \frac{Z_w}{m} & \frac{Z_q}{m} + U_0 & -g\cos\phi_0\sin\theta_0 \\ \frac{M_u}{I_{yy}} & \frac{M_w}{I_{yy}} & \frac{M_q}{I_{yy}} & 0 \\ 0 & 0 & \cos\phi_0 & 0 \end{bmatrix} \tag{3.10}$$

$$A_{\text{long/lat}} = \begin{bmatrix} \frac{X_v}{m} & \frac{X_p}{m} & \frac{X_r}{m} + V_0 & 0 \\ \frac{Z_v}{m} & \frac{Z_p}{m} - V_0 & \frac{Z_r}{m} & -g\sin\phi_0\cos\theta_0 \\ \frac{M_v}{I_{yy}} & \frac{M_p}{I_{yy}} & \frac{M_r}{I_{yy}} & 0 \\ 0 & 0 & -\sin\phi_0 & 0 \end{bmatrix} \tag{3.11}$$

$$A_{\text{lat/long}} = \begin{bmatrix} \frac{Y_u}{m} & \frac{Y_w}{m} & \frac{Y_q}{m} & -g\sin\phi_0\sin\theta_0 \\ \frac{I_{zz}L_u + I_{xz}N_u}{\Gamma} & \frac{I_{zz}L_w + I_{xz}N_w}{\Gamma} & \frac{I_{zz}L_q + I_{xz}N_q}{\Gamma} & 0 \\ \frac{I_{xz}L_u + I_{xx}N_u}{\Gamma} & \frac{I_{xz}L_w + I_{xx}N_w}{\Gamma} & \frac{I_{xz}L_q + I_{xx}N_q}{\Gamma} & 0 \\ 0 & 0 & \sin\phi_0\tan\theta_0 & 0 \end{bmatrix} \tag{3.12}$$

$$A_{\text{lat}} = \begin{bmatrix} \frac{Y_v}{m} & \frac{Y_p}{m} + W_0 & \frac{Y_r}{m} - U_0 & g\cos\phi_0\cos\theta_0 \\ \frac{I_{zz}L_v + I_{xz}N_v}{\Gamma} & \frac{I_{zz}L_p + I_{xz}N_p}{\Gamma} & \frac{I_{zz}L_r + I_{xz}N_r}{\Gamma} & 0 \\ \frac{I_{xz}L_v + I_{xx}N_v}{\Gamma} & \frac{I_{xz}L_p + I_{xs}N_p}{\Gamma} & \frac{I_{xz}L_r + I_{xx}N_r}{\Gamma} & 0 \\ 0 & 1 & \cos\phi_0\tan\theta_0 & 0 \end{bmatrix} \tag{3.13}$$

All the elements in the above matrices can be obtained through numerical perturbation. However, there are gravitational and inertial terms in the matrix that can be accurately obtained through an analytical study of the equations of motion. For this reason, these gravitational and inertial terms can serve as a good references for the sanity check once A is obtained from the linearization process. For example, the term $-g\cos\theta_0$ in the matrix A_{long} can be computed with trim pitch attitude θ_0. In another example, the term $\frac{Z_q}{m} + U_0$ in the matrix A_{long} is dominated by U_0 in forward flight.

Finally, the control matrix B is provided:

$$B = \begin{bmatrix} \frac{X_{\theta_c}}{m} & \frac{X_{\theta_{1s}}}{m} & \frac{X_{\theta_{1c}}}{m} & \frac{X_{\theta_{\mathrm{ctr}}}}{m} \\ \frac{Z_{\theta_c}}{m} & \frac{Z_{\theta_{1s}}}{m} & \frac{Z_{\theta_{1c}}}{m} & \frac{Z_{\theta_{\mathrm{ctr}}}}{m} \\ \frac{M_{\theta_c}}{I_{yy}} & \frac{M_{\theta_{1s}}}{I_{yy}} & \frac{M_{\theta_{1c}}}{I_{yy}} & \frac{M_{\theta_{\mathrm{ctr}}}}{I_{yy}} \\ 0 & 0 & 0 & 0 \\ \frac{Y_{\theta_c}}{m} & \frac{Y_{\theta_{1s}}}{m} & \frac{Y_{\theta_{1c}}}{m} & \frac{Y_{\theta_{\mathrm{ctr}}}}{m} \\ \frac{I_{zz}L_{\theta_c}+I_{xz}M_{\theta_c}}{\Gamma} & \frac{I_{zz}L_{\theta_{1s}}+I_{xz}M_{\theta_{1s}}}{\Gamma} & \frac{I_{zz}L_{\theta_{1c}}+I_{xz}M_{\theta_{1c}}}{\Gamma} & \frac{I_{zz}L_{\theta_{\mathrm{ctr}}}+I_{xz}M_{\theta_{0_{\mathrm{tr}}}}}{\Gamma} \\ \frac{I_{xz}L_{\theta_c}+I_{xx}M_{\theta_c}}{\Gamma} & \frac{I_{xz}L_{\theta_{1s}}+I_{xx}M_{\theta_{1s}}}{\Gamma} & \frac{I_{xz}L_{\theta_{1c}}+I_{xx}M_{\theta_{1c}}}{\Gamma} & \frac{I_{xz}L_{\theta_{\mathrm{ctr}}}+I_{xx}M_{\theta_{\mathrm{ctr}}}}{\Gamma} \\ 0 & 0 & 0 & 0 \end{bmatrix} \tag{3.14}$$

Besides the state (3.8), the measurement equation is also required:

$$y = Cx \tag{3.15}$$

The measurement vector y is determined by the available sensors. In the later section, controllability and observability of the resultant system ((3.8) and (3.15)) need to be determined by calculating $M = (B \ AB \ A^2B \ ... \ A^{n-1}B)$ and $O = (C \ CA \ CA^2 \ ... \ CA^{n-1})$, where n is the number of states.

Case Study for Longitudinal Motion of Helicopter at Hover

In this section, the mathematical model of a single helicopter in hover is linearized. The following Table 3.2 provides the symbols and subscripts to be used.

A helicopter model at hover, where only the longitudinal motion is considered, can be modeled in state space form as

$$\begin{aligned} \dot{x} &= f(x,u) = A(x,u)x + B(x,u)u \\ y &= Cx \end{aligned} \tag{3.16}$$

Table 3.2 Symbols and subscripts of helicopter model in hover

Symbols	Meanings
x_1, x_3	Forward, vertical displacement
x_2, x_4	Forward, vertical velocity
θ, q	Pitch angle and pitch rate
B_1	Longitudinal cyclic angle
θ_o	Collective pitch angle
w_c	Weight coefficient
x, z	Aerodynamic force derivatives
m	Aerodynamic pitch moment derivative
Subscripts	Meanings
u	Aerodynamic derivative due to forward velocity
w	Aerodynamic derivative due to vertical velocity
q	Aerodynamic derivative due to pitch rate
B_1	Aerodynamic derivative due to longitudinal cyclic angle
θ_o	Aerodynamic derivative due to pitch angle

where $x = [x_1, x_2, x_3, x_4, \theta, q]^{\mathrm{T}}$, $u = [B_1, \theta_o]^{\mathrm{T}}$, $y = [\theta, x_4]^{\mathrm{T}}$ and the state matrices A, B and C are

$$A = \begin{bmatrix} 0 & 1 & 0 & 0 & 0 & 0 \\ 0 & x_u & 0 & x_w & -w_c & x_q \\ 0 & 0 & 0 & 1 & 0 & 0 \\ 0 & z_u & 0 & z_w & 0 & z_q \\ 0 & 0 & 0 & 0 & 0 & 1 \\ 0 & m_u & 0 & m_w & 0 & m_q \end{bmatrix}$$

$$B = \begin{bmatrix} 0 & 0 \\ x_{B_1} & x_{\theta_o} \\ 0 & 0 \\ z_{B_1} & z_{\theta_o} \\ 0 & 0 \\ m_{B_1} & m_{\theta_o} \end{bmatrix}$$

$$C = \begin{bmatrix} 0 & 0 & 0 & 0 & 1 & 0 \\ 0 & 0 & 0 & 1 & 0 & 0 \end{bmatrix}$$

In particular, the aerodynamic parameters are calculated according to [9] as

$$\begin{aligned} x_u &= -2.1268\theta_o^2 + 0.0353\theta_o - 0.004 \\ x_w &= -(\theta - B_1)(5.609\theta_o^2 - 2.797\theta_o - 0.0621) \\ x_q &= 2.0074\theta_o - 0.0141 \\ x_{\theta_o} &= -(\theta - B_1)(4.3428\theta_o^2 - 2.4937\theta_o - 0.0354) \\ x_{B_1} &= 0.08185\theta_o - 0.0035 \end{aligned}$$

$$
\begin{aligned}
z_u &= 0 \\
z_w &= 5.609\theta_o^2 - 2.797\theta_o - 0.0621 \\
z_q &= 0 \\
z_{\theta_o} &= 4.3428\theta_o^2 - 2.4937\theta_o - 0.0354 \\
z_{B_1} &= 0
\end{aligned}
$$

$$
\begin{aligned}
m_u &= 233.3.64\theta_o^2 + 24.7213\theta_o + 0.4129 \\
m_w &= B_1(606.7919\theta_o^2 - 302.58\theta_o - 6.7138) \\
m_q &= -4.5622\theta_o - 0.06324 \\
m_{\theta_o} &= B_1(469.8083\theta_o^2 - 269.7760\theta_o - 3.835) \\
m_{B_1} &= -88.5473\theta_o - 11.4745
\end{aligned}
$$

$$
w_c = -0.0856
$$

The linearization of the mathematical model in (3.16) may be done by expanding the nonlinear function into a Taylor series about the operating point and neglecting the higher order terms of the expansion [74]. Considering (3.16), the equilibrium point of the system may be found by solving

$$
f(x, u) = 0 \tag{3.17}
$$

The equilibrium points are found to be at $(x_0, u_0) = (0, 0)$. This is followed by doing a Taylor series expansion of (3.16) about the equilibrium point, which results in

$$
\begin{aligned}
\dot{x} &= f(x, u) \\
&= f(x_0, u_0) + \left[\frac{\partial f}{\partial x_1}(x_1 - x_{01}) + \frac{\partial f}{\partial x_2}(x_2 - x_{02}) + \cdots + \frac{\partial f}{\partial x_6}(x_6 - x_{06}) \right. \\
&\qquad \left. + \frac{\partial f}{\partial u_1}(u_1 - u_{01}) + \frac{\partial f}{\partial u_2}(u_2 - u_{02}) \right] \\
&\quad + \frac{1}{2!} \left[\frac{\partial^2 f}{\partial x_1^2}(x_1 - x_{01})^2 + \frac{\partial^2 f}{\partial x_2^2}(x_2 - x_{02})^2 + \cdots + \frac{\partial^2 f}{\partial u_2^2}(u_2 - u_{02})^2 \right] + \cdots
\end{aligned} \tag{3.18}
$$

The partial derivatives are evaluated at the operating point, and neglecting the higher order derivatives yield

$$\dot{x} - f(x_0, u_0) = \left[\frac{\partial f}{\partial x_1}(x_1 - x_{01}) + \frac{\partial f}{\partial x_2}(x_2 - x_{02}) + \cdots + \frac{\partial f}{\partial x_6}(x_6 - x_{06}) + \frac{\partial f}{\partial u_1}(u_1 - u_{01}) + \frac{\partial f}{\partial u_2}(u_2 - u_{02}) \right]$$

It is noted that the matrix C in (3.16) is already constant and it therefore does not need to be linearized. The resulting linearized state space representation of the system is given by

$$\begin{aligned} \dot{x} &= Ax + Bu \\ y &= Cx \end{aligned} \tag{3.19}$$

where A and B are constant matrices defined as

$$A = \begin{bmatrix} \frac{\partial f_1}{\partial x_1} & \cdots & \frac{\partial f_1}{\partial x_6} \\ \vdots & \ddots & \vdots \\ \frac{\partial f_6}{\partial x_1} & \cdots & \frac{\partial f_6}{\partial x_6} \end{bmatrix} = \begin{bmatrix} 0 & 1 & 0 & 0 & 0 & 0 \\ 0 & -0.004 & 0 & 0 & -0.856 & -0.0141 \\ 0 & 0 & 0 & 1 & 0 & 0 \\ 0 & 0 & 0 & -0.0621 & 0 & 0 \\ 0 & 0 & 0 & 0 & 0 & 1 \\ 0 & 0.4129 & 0 & 0 & 0 & -0.0632 \end{bmatrix}$$

$$B = \begin{bmatrix} \frac{\partial f_1}{\partial u_1} & \frac{\partial f_1}{\partial u_2} \\ \vdots & \vdots \\ \frac{\partial f_6}{\partial u_1} & \frac{\partial f_6}{\partial u_2} \end{bmatrix} = \begin{bmatrix} 0 & 0 \\ -0.0035 & 0 \\ 0 & 0 \\ 0 & -0.0354 \\ 0 & 0 \\ -11.4745 & 0 \end{bmatrix}$$

Following the linearization of the system, the controllability and observability matrices of the resulting system are given by $M = (B \; AB \; A^2B \; ... \; A^5B)$ and $O = (C \; CA \; CA^2 \; ... \; CA^5)^{\mathrm{T}}$ are calculated using MATLAB. Both the matrices are found to have full rank of 6. This implies that the linearized system is both controllable and observable.

3.4 Description of Stability and Control Derivatives

In this section, a detailed illustration is provided on key stability and control derivatives. This description focuses on contributing sources, physical interpretation, and typical signs of these derivatives. Part of the description is a variation from [81].

- X_u: this term represents drag damping, contributed mainly from fuselage parasite drag and main rotor H-force. By definition, the sign of X_u is negative and the

magnitude grows larger as speed increases. As $X_{\mathrm{FU}} \cong -\frac{1}{2}\rho U_0^2 S_{\mathrm{ref}}$, where S_{ref} is the equivalent flat plate drag area, it follows that:

$$\frac{X_u}{m} \cong \frac{1}{m}\frac{\partial X_{\mathrm{FU}}}{\partial u} = -\frac{\rho U_0 S_{\mathrm{ref}}}{m} \tag{3.20}$$

- Z_w: heave damping. At hover, the value of Z_w determines the time constant of vertical response.
- M_u: speed stability. At hover, the rotor flaps back in response to a head wind disturbance. As the resultant nose-up moment is in the direction opposing the disturbance, the rotary-wing vehicle is statically stable with M_u being positive. However, an excessive value of M_u may lead to unstable phugoid response and is sensitive to gust. In forward flight, the rotor has a similar contribution while the horizontal stabilizer (if mounted) may have a significant effect to M_u depending on the location of the stabilizer. If the horizontal stabilizer is mounted directly under the main rotor and experiences download from rotor downwash, it enhances M_u. If the horizontal stabilizer experiences upload during flight, the effect is destabilizing.
- M_w: angle of attack stability. At hover, the value of M_w is close to zero. In forward flight, a positive increase of angle of attack leads to backward tilting of the rotor, creating a nose-up moment to further increase the angle of attack. Thus, the contribution from the rotor to M_w is destabilizing with its corresponding value taking positive sign. A horizontal stabilizer (whether it experiences download or upload) contributes a stabilizing effect, which is the main reason to justify its existence in a pure helicopter configuration. In addition, a forward C.G. location (ahead of rotor shaft) will contribute a stabilizing moment.
- M_q: pitch damping. For a rotor with counter clockwise rotation, a positive change in the pitch rate results in a negative roll due to gyroscopic moment. This in turn causes a flap-down for the blade over the nose and a flap-up for the blade over the tail. The resultant nose-down moment opposes the original pitch rate variation, thus the damping effect. In fact, the above explanation can be referred to (2.16):

$$\beta_{1c} = -\frac{16}{\gamma\Omega} q_{\mathrm{H}} \tag{3.21}$$

  Another interesting interpretation of the above equation is that when the fuselage is tilting at a constant pitch rate q_{H}, the time lag between the fuselage and the rotor is $\frac{16}{\gamma\Omega}$ s.
- L_v: Dihedral effect. L_v is the lateral counterpart of M_u. For a right sideslip, the rotor responds with a left roll. A positive dihedral effect thus takes a negative value. The contributions from both tail rotor and vertical tail depend on their relative location above or below C.G. When above C.G., the effect is stabilizing and *vice versa*. Similar to M_u, an excessively large value of L_v may not be preferable. In some helicopter configurations, the vertical tail is placed underneath the tail boom in order to have a moderate value of L_v.

- L_p: roll damping. L_p is the lateral counterpart of M_q. Again, from (2.16), it follows that:

$$\beta_{1s} = -\frac{16}{\gamma\Omega} p_{\mathrm{H}} \tag{3.22}$$

- N_v: weathercock stability. The main contributions to N_v are from the tail rotor and vertical tail. Both are stabilizing with N_v taking a positive value.
- M_p and L_q: cross-coupling due to roll/pitch rates. Once again, (2.16) can be used:

$$\beta_{1s} = -\frac{q_{\mathrm{H}}}{\Omega} \tag{3.23}$$

$$\beta_{1c} = \frac{p_{\mathrm{H}}}{\Omega} \tag{3.24}$$

  Thus, M_p takes a positive value while L_q is negative.
- Z_{θ_c}, $M_{\theta_{1s}}$, $L_{\theta_{1c}}$, and $N_{\theta_{\mathrm{ctr}}}$: collective/pitch/roll/yaw control power.

In the subsequent sections, three examples will be provided on linearized dynamics for the rotary-wing aircraft. The first two examples deal with two different hobby helicopters (Yamaha R50 and Copterwork AF25B) at two different flight conditions (hover and forward flight). The last example illustrates a combined system consisting of a helicopter and an underslung load.

3.5 Yamaha R50 Helicopter at Hover

Consider the longitudinal linearized model of the Yamaha R50 helicopter [54] at hover:

$$\begin{bmatrix} \dot{u} \\ \dot{w} \\ \dot{q} \\ \dot{\theta} \end{bmatrix} = \begin{bmatrix} -0.0553 & 0.0039 & 1.413 & -32.1731 \\ -0.0027 & -0.5727 & -0.0236 & -\ 0.2358 \\ 0.2373 & 0.002 & -6.9424 & 0 \\ 0 & 0 & 1 & 0 \end{bmatrix} \begin{bmatrix} u \\ w \\ q \\ \theta \end{bmatrix} + \begin{bmatrix} 11.2579 & 0 \\ 0.0698 & -0.199 \\ -38.6267 & 0 \\ 0 & 0 \end{bmatrix} \begin{bmatrix} \delta \\ \delta_\Omega \end{bmatrix} \tag{3.25}$$

where δ is longitudinal cyclic control and δ_Ω denotes the main rotor RPM variation.

It is interesting to compare the state matrix in (3.25) and A_{long} in (3.10). Although trim roll and pitch attitudes are not provided in [54], their values can be assumed to be small. Therefore, the two gravitational terms, $-g\cos\theta_0$ and $-g\cos\phi_0\sin\theta_0$,

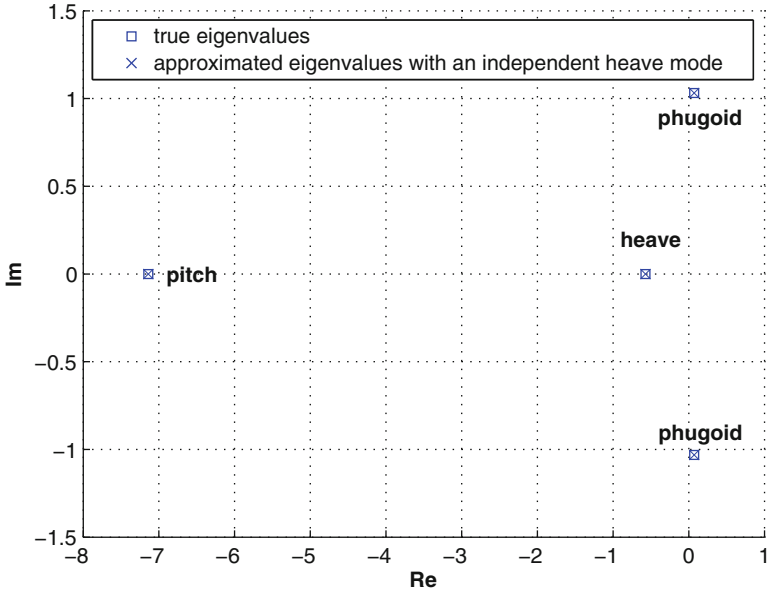

Fig. 3.1 Eigenvalue plot for Yamaha R50 helicopter at hover

take estimated values of $-32.2\ ft/s^2$ and $0\ ft/s^2$, respectively. By the same token, the kinematic term $\cos\phi_0$ is close to 1. Moreover, some terms are weak at hover, including X_u, X_w, Z_u, Z_q, and M_w. The term X_q is drag due to pitch rate with the main contribution from main rotor. Following a positive change in pitch rate, the main rotor with a counter-clockwise rotation has a tendency of left roll due to gyroscopic moment, which results in a forward tilting of the rotor disk. Thus, the sign of X_q should be positive. In fact, this process is how the opposing pitch-down moment is generated for the pitch damping M_q. Due to hingeless rotor configuration for the R50 helicopter, the value of M_q is fairly large if compared to normal articulated or even teetering rotor configurations. The magnitude of M_q can also take the contribution from the fly bar. The positive sign of M_u has already been discussed in the last section. Thus, the state matrix in (3.25) appears to be reasonable from the above sanity check.

From the given linearized dynamics in (3.25), a distribution of eigenvalues can be obtained (see Fig. 3.1). An approximation can be made by further assuming that the heave dynamics are independent from the remaining dynamics. From the figure, it can be seen that the differences in eigenvalues from both approximated dynamics and full dynamics are indiscernible. This is not surprising as the rotor is aerodynamically symmetric at hover condition. It also shows that the heave mode at hover can be characterized as a first-order dynamic system with time constant at 1.75 s.

Apart from heave mode, the remaining eigenvalues include one pair of complex conjugates, often known as the phugoid mode, and one at real axis, known as the pitch mode. While the pitch mode is stable and aperiodic, the phugoid mode here is mildly unstable and oscillatory.

Going back to matrix A_{long}, it reduces to the following form when taking out the heave dynamics [81]:

$$A_{\text{long,reduced}} = \begin{bmatrix} \frac{X_u}{m} & \frac{X_q}{m} & -g \\ \frac{M_u}{I_{yy}} & \frac{M_q}{I_{yy}} & 0 \\ 0 & 1 & 0 \end{bmatrix} \tag{3.26}$$

The corresponding characteristic equation is

$$s^3 - \left(\frac{X_u}{m} + \frac{M_q}{I_{yy}}\right) s^2 + \left(\frac{X_u}{m}\frac{M_q}{I_{yy}} - \frac{M_u}{I_{yy}}\frac{X_q}{m}\right) s + \frac{M_u}{I_{yy}} g = 0 \tag{3.27}$$

When $M_u = 0$, the resulting characteristic equation will have three roots on the real axis: 0, X_u/m, and M_q/I_{yy}. When the value of M_u/I_{yy} is increased from 0 to 0.2373, it can be found that the root close to M_q/I_{yy} hardly moves, while the root locus corresponding to 0 and X_u/m first merges together on the real axis before becoming a complex pair and moving towards the right half of the plane. The result is shown in Fig. 3.2.

Figure 3.2 indicates that the eigenvalue associated with the pitch mode is mainly determined by M_q, and an increase in value of M_u may result in an unstable phugoid mode.

It is also interesting to discuss the effect of M_q. The results from M_q variation can be seen in Fig. 3.3. There are three values of M_q: original value, half of the original value, and double of the original value. From the figure, it is clear that increasing pitch damping is beneficial to the system stability.

As a side note, the lateral linearized dynamics is a mirror image of longitudinal counterpart due to the main rotor's aerodynamic symmetry at hover. Similar to longitudinal dynamics, there are three modes in lateral dynamics: yaw mode, roll mode, and dutch roll model. The correspondence between the two dynamics are: heave mode vs. yaw mode, pitch mode vs. roll mode, and phugoid mode vs. dutch roll mode.

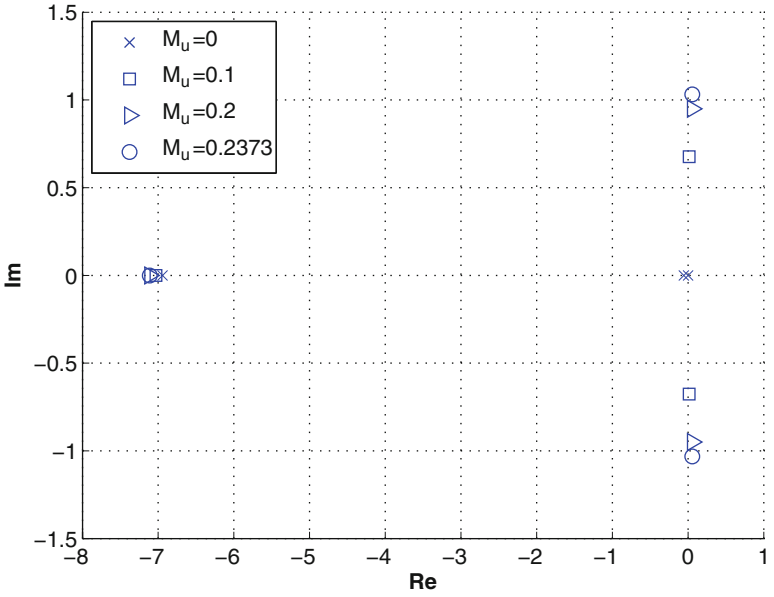

Fig. 3.2 Influence of speed stability M_u

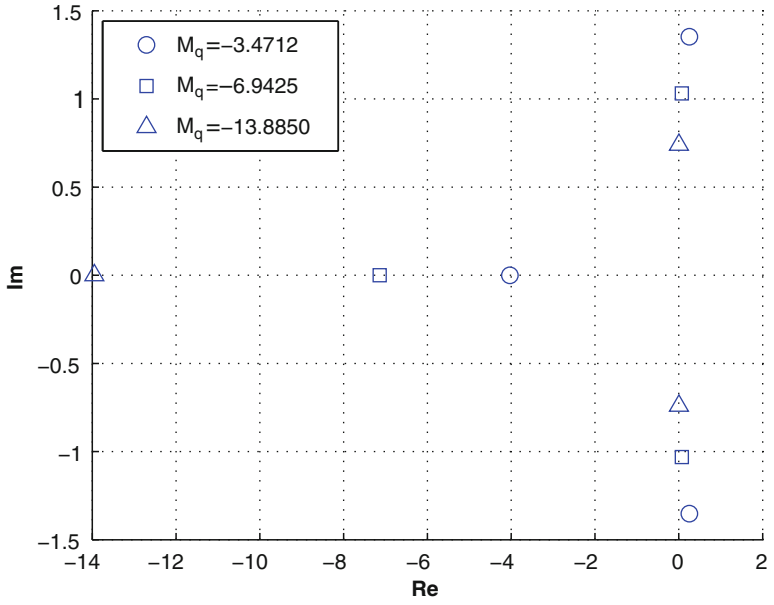

Fig. 3.3 Influence of pitch damping M_q

3.6 Copterworks AF25B Helicopter in Forward Flight

Due to aerodynamic asymmetry on the main rotor in forward flight and dynamic coupling from the flapping blades and constantly spinning rotor, longitudinal and lateral dynamics may not always be sufficiently decoupled. This is added complexity when compared to the analysis of fixed-wing aircraft.

In this section, a coupled linearized model for a Copterworks AF25B radio control helicopter is analyzed (see Fig. 3.4). The condition is straight level flight at 40 knots. The gross weight of the helicopter is 30 kg. Trimmed roll and pitch attitudes are 1.43° and −10.2°, respectively. Velocities along the body x-axis and z-axis are $U_0 = 66.4915$ and $W_0 = -11.9628$. The linearized model is shown in (3.28):

$$A = \begin{bmatrix} -0.1634 & 0.0676 & 14.1039 & -31.6911 \\ -0.0792 & -0.9827 & 73.9560 & 5.6832 \\ 0.0208 & 0.1940 & -24.1599 & -0.0014 \\ 0 & 0 & 0.9997 & 0 \\ -0.0014 & -0.0046 & -1.6321 & 0.1414 \\ 0.3740 & 0.2245 & -106.5635 & 0.0010 \\ 0.0272 & 0.0304 & -0.2059 & 0 \\ 0 & 0 & -0.0045 & -0.0001 \end{bmatrix}$$

$$\begin{bmatrix} -0.0029 & -1.8475 & -1.4723 & 0.0003 \\ 0.0314 & 2.4586 & -0.4810 & -0.7882 \\ 0.1118 & 41.7746 & -0.0236 & -0.0127 \\ 0 & 0 & -0.0249 & 0.0001 \\ -0.0804 & -14.0134 & -66.2104 & 31.6828 \\ -0.3005 & -67.5186 & -0.1599 & 0.0049 \\ 0.1869 & 0.6160 & -0.8763 & 0 \\ 0 & 1.0000 & -0.1793 & -0.0001 \end{bmatrix} \tag{3.28}$$

Once again, a sanity check of the state matrix is in order. In the follow-up discussion, entry (n,m) stands for n^{th} row and m^{th} column.

1. Entry (1,1): drag damping X_u. In the nonlinear modeling, equivalent flat-plate drag area is assumed to be $2 ft^2$. Based on (3.20), X_u is estimated at −0.1577, a value close to −0.1634 from the linearization.
2. Entry (1,3): $X_q - W_0$. This term is dominated by vertical speed along the body z-axis $-W_0$.
3. Entries (1,4), (2,4), (2,8), (5,4), (5,8): gravitational terms. The calculated values based on corresponding entries in (3.8) are −31.6843, 5.6999, −0.7908, 0.1423, and 31.6813, sufficiently close to corresponding entries in the state matrix.

Fig. 3.4 AF25B radio control helicopter from Copterworks(Courtesy of Copterworks Inc.)

4. Entry (2,2): heave damping Z_w. At hover, $Z_w = -0.4$ for AF25B. The magnitude of Z_w tends to increase with higher speed [78].
5. Entry (2,3): $Z_q + U_0$. This term is dominated by forward speed along the body x-axis U_0.
6. Entry (3,1): speed stability M_u. In reference to M_u for Lynx helicopter (see Fig. 4.15 of [78]), the value of M_u is reduced with the increase of speed from hover to moderate speed. The value of M_u is 0.0825 at hover for the AF25B, decreasing to 0.0208 at 40 knots. This comparison is reasonable since both the AF25B and the Lynx have hingeless rotor configurations.
7. Entry (3,2): angle of attack stability M_w. The positive value here indicates the destabilizing effect of M_w. This is because the AF25B has no horizontal stabilizer to produce opposing pitching moment from a variation of vertical velocity.
8. Entries (3,3) and (6,6): pitch damping term M_q and roll damping term L_p. Both values are negative. Compared to the value in entry (3,3), the one in entry (6,6) is almost three times larger. This is due to roll moment of inertia I_x which is three times less than the pitch moment of inertia I_y.
9. Entries (3,6) and (6,3): cross-coupling M_p and L_q. The signs are positive for M_p and negative for L_q, which conform to the analysis in Sect. 3.4.
10. Entries (4,3), (4,7), (8,3), (8,7): kinematic terms. The calculated values based on corresponding entries in (3.8) are 0.9997, −0.0250, −0.0045, and −0.1799, which are in good agreement with corresponding entries in the state matrix.
11. Entry (6,5): dihedral effect L_v. Here, the negative value has a stabilizing effect, which mainly comes from the main rotor. However, it should be noted that the effect from the vertical fin is destabilizing as the fin is mounted below the C.G..
12. Entry (7,5): weathercock effect N_v. As expected, the value of N_v in the state matrix is positive with main contributions from the tail rotor and vertical fin.

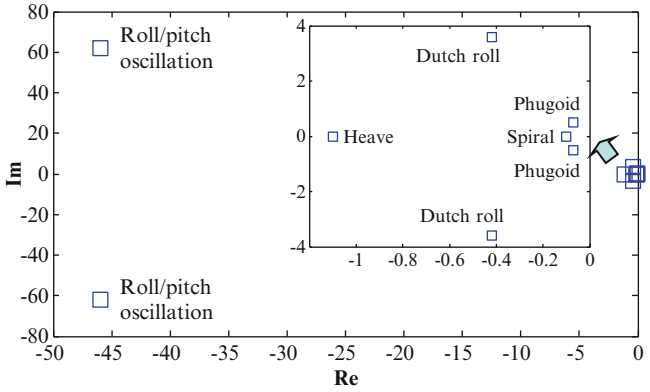

Fig. 3.5 Eigenvalue distribution for the AF25B at 40 knots

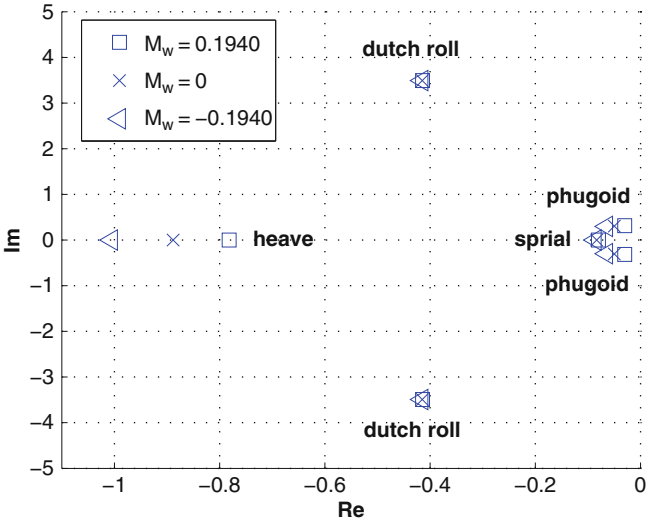

Fig. 3.6 Variation of M_w on the eigenvalue distribution

Following the sanity check on the state matrix, the corresponding eigenvalues are plotted in Fig. 3.5. Far away to the imaginary axis in the left half of the complex plane is the roll/pitch oscillation mode. Mainly due to the hingeless rotor configuration and its associated large hub moment, the dynamics of this mode are rapid. Other modes are all close to the imaginary axis and stable, including heave, spiral, dutch roll, and phugoid modes. In particular, the phugoid mode is the closest to the imaginary axis, indicating minimum stability margin. An improvement on M_w is preferable (see Fig. 3.6), with the corresponding means ranging from the addition of horizontal stabilizer to forward C.G. (ahead of rotor thrust vector).

3.7 Conclusion

Stability analysis for the rotary-wing aircraft starts with trim to establish steady state condition, progresses with linearization to obtain linearized model with respect to the established trim condition, and centers on static and dynamic stability studies. Static stability provides clues on the system's initial response, while dynamic stability looks at the system behavior in the long term.

The importance of stability analysis cannot be over-estimated as it provides insights to the system characteristics and is itself the basis of flight control system design. In the subsequent chapters, several advanced control schemes will be offered for helicopter systems.